






# Cholinergic neurons in the pedunculo pontine tegmental nucleus modulate breathing in rats by direct projections to the retrotrapezoid nucleus

Janayna D. Lima<sup>1,\*</sup> , Cleyton R. Sobrinho<sup>1,\*</sup> , Barbara Falquetto<sup>2</sup>, Leonardo K. Santos<sup>1</sup>, Ana C. Takakura<sup>2</sup> , Daniel K. Mulkey<sup>3</sup>  and Thiago S. Moreira<sup>1</sup> 

<sup>1</sup>Department of Physiology and Biophysics, University of São Paulo, São Paulo, SP, Brazil

<sup>2</sup>Department of Pharmacology, University of São Paulo, São Paulo, SP, Brazil

<sup>3</sup>Department of Physiology and Neurobiology, University of Connecticut, Storrs, CT, USA

Edited by: Scott Powers & Gregory Funk

## Key points

- Cholinergic projections from the pedunculo pontine tegmental nucleus (PPTg) to the retrotrapezoid nucleus (RTN) are considered to be important for sleep–wake state-dependent control of breathing.
- The RTN also receives cholinergic input from the postinspiratory complex.
- Stimulation of the PPTg increases respiratory output under control conditions but not when muscarinic receptors in the RTN are blocked.
- The data obtained in the present study support the possibility that arousal-dependent modulation of breathing involves recruitment of cholinergic projections from the PPTg to the RTN.

**Abstract** The pedunculo pontine tegmental nucleus (PPTg) in the mesopontine region has important physiological functions, including breathing control. The PPTg contains a variety of cell types, including cholinergic neurons that project to the rostral aspect of the ventrolateral medulla. In addition, cholinergic signalling in the retrotrapezoid nucleus (RTN), a region that contains neurons that regulate breathing in response to changes in  $\text{CO}_2/\text{H}^+$ , has been shown to activate chemosensitive neurons and increase inspiratory activity. The present study aimed to identify the source of cholinergic input to the RTN and determine whether cholinergic signalling in this region influences baseline breathing or the ventilatory response to  $\text{CO}_2$  in conscious male Wistar rats. Retrograde tracer Fluoro-Gold injected into the RTN labelled a subset of cholinergic PPTg neurons that presumably project directly to the chemosensitive region of the RTN. In unrestrained awake rats, unilateral injection of the glutamate (10 mM/100 nL) in the PPTg decreased tidal volume ( $V_T$ ) but otherwise increased respiratory rate ( $f_R$ ) and net respiratory

**Janayna D. Lima** has a degree in Physical Therapy obtained in 2014 from Paraíba State University (UEPB), Brazil. Currently, she is a PhD student in the Physiology Program at the Institute of Biomedical Science, University of São Paulo (ICB-USP), working under the supervision of Dr Thiago S. Moreira. She works on central mechanisms of breathing control with emphasis on the cholinergic system. **Cleyton R. Sobrinho** obtained a Master degree in Morphology (2011) and PhD in Physiology (2015), both from the University of São Paulo (ICB-USP). For 2 years, he was Visitor Researcher in the University of Connecticut, working in brain slice patch clamping (2013 and 2017). Currently, he is a postdoctoral fellow at the ICB-USP working on central mechanisms of cardiorespiratory control, with an emphasis on purinergic and cholinergic signalling.



\*These authors contributed equally to this work.

output as indicated by an increase in ventilation ( $V_E$ ). All respiratory responses elicited by PPTg stimulation were blunted by prior injection of methyl-atropine (5 mM/50–75 nL) into the RTN. These results show that stimulation of the PPTg can increase respiratory activity in part by cholinergic activation of chemosensitive elements of the RTN. Based on previous evidence that cholinergic PPTg projections may simultaneously activate expiratory output from the pFRG, we speculate that cholinergic signalling at the level of RTN region could also be involved in breathing regulation.

(Resubmitted 28 December 2018; accepted after revision 4 February 2019; first published online 6 February 2019)

**Corresponding author** Thiago S. Moreira: Department of Physiology and Biophysics, Institute of Biomedical Science, University of São Paulo, Av. Prof. Lineu Prestes, 1524, 05508-000, São Paulo, SP, Brazil  
E-mail: tmoreira@icb.usp.br

## Introduction

The cholinergic system has been implicated in several aspects of the neurophysiology of breathing, including respiratory motor output control (Burton *et al.* 1994; Shao & Feldman, 2009; Boutin *et al.* 2017), state-dependent modulation of breathing (Kubin & Fenik, 2004) and chemosensory control of breathing (Metz, 1966; Dev & Loeschcke, 1979; Fukuda & Loeschcke, 1979; Nattie *et al.* 1989; Monteau *et al.* 1990; Sobrinho *et al.* 2016). Neuroanatomical evidence suggests that descending cholinergic projections to the ventrolateral medulla arise from neurons in the pedunculopontine tegmental nucleus (PPTg) and, to a lesser extent, from the laterodorsal tegmental nucleus (LDTg). However, medullary cholinergic neurons and the recently discovered post-inspiratory complex (PiCO) may also be sources of cholinergic input the ventrolateral medulla (Ruggiero *et al.* 1990; Yasui *et al.* 1990; Anderson *et al.* 2016).

The rostral aspect of the ventrolateral medulla contains two neighboring regions involved in breathing regulation; the parafacial respiratory group (pFRG) and the retrotrapezoid nucleus (RTN) (Guyenet & Bayliss, 2015; Del Negro *et al.* 2018; Huckstepp *et al.* 2018). The pFRG appears to be a conditional expiratory oscillator and the RTN provides an excitatory drive for both inspiration and expiration for which its activity depends on  $\text{CO}_2/\text{H}^+$  signals (Guyenet & Bayliss, 2015; Del Negro *et al.* 2018). Recent evidence suggest that ACh is released by cholinergic terminals on the ventral medullary surface (Huckstepp *et al.* 2016). Therefore, it is possible that endogenous release of ACh regulates activity of pFRG neurons and/or chemosensitive RTN neurons. Consistent with this, ACh has been shown to stimulate both pFRG (Boutin *et al.* 2017) and chemosensitive RTN neurons (Sobrinho *et al.* 2016) to regulate expiratory and inspiratory drive, respectively. Evidence also suggests cholinergic signalling via muscarinic receptors in the RTN contributes to the  $\text{CO}_2/\text{H}^+$ -dependent drive to breathe *in vivo* (Dev & Loeschcke, 1979; Nattie *et al.* 1989); however,

blockade of muscarinic receptors minimally affected  $\text{CO}_2/\text{H}^+$ -sensitivity of RTN chemoreceptors *in vitro* (Sobrinho *et al.* 2016).

These results suggest that cholinergic modulation of the RTN contributes to basal respiratory drive; however, the relative contribution of cholinergic signalling in the RTN across different states of arousal has not been characterized. Furthermore, a dense cholinergic terminal field is present within the ventrolateral medulla (Boutin *et al.* 2017), although the source of this cholinergic input remains poorly defined. In the present study, we use standard physiology and anatomical approaches to address the following questions: (i) does ACh signalling in the RTN differentially regulate breathing in anesthetized and awake unrestrained rats; (ii) what is the main source of cholinergic drive to RTN; and (iii) does the PPTg send excitatory cholinergic projections to RTN to modulate breathing by a muscarinic receptor dependent mechanism? By answering these questions, we consider that our data identify key components of the PPTg–RTN pathway, and suggest an important role of this pathway in the control of breathing.

## Methods

### Ethical approval

All experiments were conducted using male Wistar rats (weighing 250–350 g at the time of experimentation) in accordance with NIH Guide for the Care and Use of Laboratory Animals and approved by the Animal Experimentation Ethics Committee of the Institute of Biomedical Sciences at the University of São Paulo (ICB/USP; approval ref. no. 81/2015 ICB/USP). The study complied with the ethical principles of *The Journal of Physiology* and the experiments complied with The Journal's animal ethics principles and regulation checklist (Grundy, 2015). Male Wistar rats were obtained from the Rats Resource Center of the ICB/USP.

## Surgical procedures

**Anatomical experiments.** Tracer injections were made while the rats were anaesthetized with a mixture of ketamine (100 mg kg<sup>-1</sup>) and xylazine (7 mg kg<sup>-1</sup>) administered *i.p.* Surgery used standard methods as described previously in our laboratory (Barna *et al.* 2014; Silva *et al.* 2016a). After surgery, the rats were treated with the antibiotic ampicillin (30,000 IU) given *i.m.* and the analgesic Ketoflex (ketoprofen 1%, 0.03 mL per rat, *s.c.*; BioFarm, Jaboticalbal, SP, Brazil).

A group of four rats received unilateral injections of the anterograde tracer *Phaseolus vulgaris*-leucoagglutinin (PHA-L) (2.5% in 0.1 M phosphate buffer; Vector Laboratories, Burlingame, CA, USA) into the PPTg region. The tracer was delivered by iontophoresis through a glass micropipette with an internal tip diameter of 10–15  $\mu$ m, by passing a positive-pulsed current of 5  $\mu$ A and 7 s in duration every 7 s for 20 min. These injections were placed stereotaxically using the co-ordinates: 6.6 mm below the dorsal surface of the brain, 1.7 mm lateral to the midline and 7.9 mm caudal to bregma. These rats were allowed to survive 15 days following the tracer injection and then were anaesthetized with pentobarbital (60 mg kg<sup>-1</sup> *i.p.*) and perfused transcardially with fixative as described below.

Another group of four rats received an iontophoretic injection (7  $\mu$ A positive current pulses of 7 s in duration every 7 s for 15 min) of the retrograde Fluoro-Gold (FG 2%) (Fluorochrome Inc., Denver, CO, USA) into the RTN using a glass micropipette with an internal tip diameter of 18–20  $\mu$ m. These injections were made using the co-ordinates: 2.5 mm caudal to lambda, 1.8 mm lateral to the midline and 8.3 mm below the dura mater. Seven to 10 days after the FG injection, rats were anaesthetized with pentobarbital (60 mg kg<sup>-1</sup> *i.p.*), perfused transcardially and immediately perfusion-fixed.

**Physiological experiments.** Rats were anaesthetized with intraperitoneal injection of ketamine (100 mg kg<sup>-1</sup>) combined with xylazine (7 mg kg<sup>-1</sup>) and placed in a stereotaxic frame (model 900; David Kopf Instruments, Tujunga, CA, USA). Stainless steel cannulas were placed uni- or bilaterally into the RTN using the co-ordinates 2.5 mm caudal to lambda, 1.8 mm lateral to the midline and 7.5 mm below dura mater. As a control experiment, cannulas were placed into the C1/Böttinger region using the co-ordinates 2.8 mm caudal to lambda, 1.8 mm lateral to midline and 7.2 mm below the dura mater. To evaluate the effect of glutamatergic stimulation of PPTg in awake rats, stainless steel cannulas were placed unilaterally into the PPTg using the co-ordinates: 7.9 mm caudal to bregma, 1.7 mm lateral to the midline and 5.2 mm below the dura mater. In animals where there was simultaneous implantation of cannula towards the RTN and PPTg, an angle of 30° was used to implant the cannula toward the

RTN. In these animals, cannulas were placed into the RTN using the co-ordinates: 7.4 caudal to lambda, 1.8 mm lateral to the midline and 5.4 mm below from bone surface. The cannulas were fixed to the cranium using dental acrylic resin and jeweler screws. Rats received a prophylactic dose of penicillin (30,000 IU) given *i.m.* and a *s.c.* injection of the analgesic Ketoflex (1%; 0.03 mL per rat) postsurgically. After the surgery, the rats were maintained in individual boxes with free access of tap water and food pellets.

At the RTN group, 1 day before the experiment, under *i.p.* injection of ketamine (100 mg kg<sup>-1</sup>) combined with xylazine (7 mg kg<sup>-1</sup>) anaesthesia, a polyethylene tubing (PE-10 connected to PE-50; Scientific Commodities, Lake Havasu City, AZ, USA) was inserted into the abdominal aorta through the femoral artery. The cannula was tunnelled *s.c.* to the back of the rats to allow access in unrestrained, freely moving rats. This cannula was used later to measure pulsatile arterial pressure, mean arterial pressure (MAP) and heart rate (HR) in the unanaesthetized awake state, as described previously (Takakura *et al.* 2014; Barna *et al.* 2016).

**Electrophysiology preparatory surgery.** Surgical procedures were similar to those reported previously by our laboratory (Wenker *et al.* 2012; Sobrinho *et al.* 2014). Briefly, general anaesthesia was induced by the addition of 5% of halothane in 100% oxygen. The rats were tracheostomized and connected to artificial ventilator pump, and then the halothane level was reduced to 1.5–2% and maintained until the end of surgery. The femoral artery and vein were cannulated by polyethylene tubes (polyethylene tubing: outer diameter 0.6 mm, inner diameter 0.3 mm; Scientific Commodities, Lake Havasu City, AZ, USA) for measurement of pulsatile arterial pressure, MAP and for administration of fluids and drugs, respectively. Rats were adapted to stereotaxic apparatus and a capillary containing glutamate was placed into the PPTg through the trepanning of parietal bone.

The diaphragm muscle was accessed by an abdominal incision and the genioglossus muscle by the lingual retraction. Bipolar electrodes were inserted on the muscles and connected to the apparatus. At the end of the surgical procedures, halothane was replaced by urethane (1.2 g kg<sup>-1</sup>) administered slowly *i.v.* Rectal temperature was maintained at 37°C. End-tidal CO<sub>2</sub> (etCO<sub>2</sub>) was monitored throughout each experiment with a capnometer (CWE, Inc., Ardmore, PA, USA).

## *In vivo* recordings of physiological variables

One week after the stereotaxic surgery or 24 h after arterial cannulation, when the rats were recovered from the surgeries and adapted to the environment of the recording room, the arterial catheter was connected to

a pressure transducer (MLT844; ADInstruments, Sydney, NSW, Australia) coupled to a preamplifier (Bridge Amp, ML221; ADInstruments) that was preconnected to a Powerlab computer data acquisition system (PowerLab 16/30, ML880; ADInstruments).

Whole-body plethysmography was used to measure respiratory activity in awake and, 24 h later, in urethane-anaesthetized rats. Adult rats were placed individually into a plexiglass recording chamber (5 L) that was flushed continuously with a mixture of 79% nitrogen and 21% oxygen (unless otherwise required by the protocol) at a rate of 1.3 L min<sup>-1</sup>. A volume calibration was performed during each experiment by injecting a known air volume (1 mL) inside the chamber. All experiments were performed at room temperature (24–26 °C).

Tidal volume ( $V_T$ , measured in mL, normalized to body weight and corrected to account for chamber and animal temperature, humidity, and atmospheric pressure) and respiratory frequency ( $f_R$ , breaths min<sup>-1</sup>) were recorded on a breath-to-breath basis and analysed during the last two minutes of each experimental condition when breathing was stabilized; the product of tidal volume and frequency is minute ventilation ( $V_E$ , mL min<sup>-1</sup> g<sup>-1</sup>). Measurements of breathing activity were performed using a whole-body plethysmography-closed system as described previously by Drorbaugh and Fenn (1955).

Concentrations of O<sub>2</sub> and CO<sub>2</sub> in the chamber were monitored online using a fast-response O<sub>2</sub>/CO<sub>2</sub> monitor (ADInstruments). The pressure signal was amplified, filtered, recorded and analysed offline using Powerlab software (Powerlab 16/30, ML880/P; ADInstruments).

### Electrophysiology recording

MAP, diaphragm (DIA<sub>EMG</sub>), genioglossal (GG<sub>EMG</sub>) and etCO<sub>2</sub> were recorded. They were digitalized with a micro1401 (Cambridge Electronic Design, Cambridge, UK), stored on a computer, and processed offline with Spike 2, version 6 (Cambridge Electronic Design) (Takakura & Moreira, 2011). Integrated DIA<sub>EMG</sub> and GG<sub>EMG</sub> were obtained after rectification and smoothing ( $\tau = 0.015$  s) of the original signal, which were acquired with a 30–300 Hz bandpass filter.

### Chemoreflex analysis

Conscious rats were allowed at least 30–45 min to acclimatize to the chamber environment at normoxia/normocapnia (21% O<sub>2</sub>, 79% N<sub>2</sub> and <0.5% CO<sub>2</sub>) before measurements of baseline MAP and ventilation were taken. Hypercapnia was induced by titrating CO<sub>2</sub> into the respiratory mixture up to a level of 8–10% for 10 min.

### Drugs

All drugs were purchased from Sigma-Aldrich (St Louis, MO, USA), unless otherwise stated. For *in vivo* experiments, ACh (ACh: 10 mM in sterile saline, pH 7.4; 50 nL), methyl-atropine (M-Atr: 5 mM in sterile saline, pH 7.4; 50–75 nL), glutamate (10 mM in sterile saline, pH 7.4; 100 nL) or kynurenic acid (kyn: 100 mM in sterile saline, pH 7.4; 50–75 nL) was injected uni- or bilaterally using a 1 or 5  $\mu$ L Hamilton syringe connected to an injection needle positioned in the guide cannula (the tip of the needle extended 1.5–3.5 mm beyond the end of the cannula).

### Experimental protocols

#### Respiratory and cardiovascular effects produced by injection of M-Atr and ACh into the RTN in conscious rats.

$V_T$  (mL kg<sup>-1</sup>),  $f_R$  (breaths min<sup>-1</sup>),  $V_E$  (mL kg<sup>-1</sup> min<sup>-1</sup>) and MAP (mmHg) were continuously recorded during 2 min, starting 30–45 min after the rats were placed individually into a plexiglass recording chamber. Control (baseline) values were recorded for 2 min and were analysed immediately before the first treatment (saline or M-Atr into the RTN). These values were used as reference to calculate the changes produced by the treatments. ACh (10 mM/50 nL) or saline was injected unilaterally into the RTN 10 min after the unilateral injection of M-Atr (5 mM/50–75 nL) or saline in the same place. Four groups of rats were used to investigate the respiratory and cardiovascular effects produced by the combination of RTN injections of M-Atr or saline and ACh or saline:

- (1) Saline into the RTN followed by saline into the RTN (control group – resting condition);
- (2) Saline into the RTN followed by ACh into the RTN;
- (3) M-Atr into the RTN followed by saline into the RTN;
- (4) M-Atr into the RTN followed by ACh into the RTN.

#### Respiratory responses to hypercapnia in conscious or anaesthetized rats treated with M-Atr into the RTN.

$V_T$  (mL kg<sup>-1</sup>),  $f_R$  (breaths min<sup>-1</sup>) and  $V_E$  (mL kg<sup>-1</sup> min<sup>-1</sup>) were continuously recorded during 2 min, starting 30–45 min after the rats were placed individually into a plexiglass recording chamber. Control (baseline – normoxia condition) values were recorded for 2 min and were analysed immediately before the exposure to high levels of CO<sub>2</sub> (hypercapnia: 7% CO<sub>2</sub>, 21% O<sub>2</sub> and balance N<sub>2</sub>). These values were used as reference to calculate the changes produced by the hypercapnia challenge. M-Atr (5 mM/50–75 nL) or saline was injected bilaterally into the RTN and 10 min later, respiratory parameters were evaluated under normoxia

and hypercapnia conditions. Two groups of rats were used:

- (1) Saline into the RTN (control group);
- (2) M-Atr into the RTN.

Twenty-four hours later, we used the same groups of animals to evaluate the hypercapnic ventilatory response in urethane-anaesthetized rats with bilateral injection of saline or M-Atr into the RTN.

**Respiratory and cardiovascular effects produced by injection of glutamate into PPTg in anaesthetized rats.** MAP,  $\text{DIA}_{\text{EMG}}$ ,  $\text{GG}_{\text{EMG}}$  and  $\text{etCO}_2$  were continuously recorded through the entire experimental protocol. Before starting the experiments, the ventilation was adjusted to have the  $\text{etCO}_2$  at 3–4% at steady-state (60–80 cycles  $\text{s}^{-1}$ ; tidal volume 1–1.2 mL/100 g). Control (baseline) values were recorded for 2 min and were analysed immediately before the first treatment [saline or glutamate (10 mM/100 nL) into the PPTg]. These values were used as reference to calculate the changes produced by the treatments. Two groups of rats were used to investigate the respiratory and cardiovascular effects produced by the unilateral injection of glutamate or saline into the PPTg:

- (1) Saline into the PPTg (control group);
- (2) Glutamate into the PPTg.

**Respiratory effects produced by injection of M-Atr or kyn into the RTN and glutamate into the PPTg in conscious rats.**  $V_T$  (mL  $\text{kg}^{-1}$ ),  $f_R$  (breaths  $\text{min}^{-1}$ ) and  $V_E$  (mL  $\text{kg}^{-1}$   $\text{min}^{-1}$ ) were continuously recorded during 2 min, starting 30–45 min after the rats were placed individually into a plexiglass recording chamber. Control (baseline) values were recorded for 2 min and were analysed immediately before the first treatment (saline or M-Atr into the RTN) or (vehicle or kyn into the RTN). These values were used as reference to calculate the changes produced by the treatments. Glutamate (10 mM/100 nL) or saline was injected unilaterally into the PPTg 10 min after the unilateral injection of M-Atr (5 mM/50–75 nL) (Furuya *et al.* 2014) or saline or kyn (100 mM/50–75 nL) or vehicle in RTN. Six groups of rats were used to investigate the respiratory effects produced by the combination of PPTg and RTN injections:

- (1) Saline into the RTN followed by saline into the PPTg (control group);
- (2) Saline into the RTN followed by glutamate into the PPTg;
- (3) M-Atr into the RTN followed by saline into the PPTg;
- (4) M-Atr into the RTN followed by glutamate into the PPTg;
- (5) Kyn into the RTN followed by saline into the PPTg;

- (6) Kyn into the RTN followed by glutamate into the PPTg;

## Histology

At the end of the experiments, rats were deeply anaesthetized with pentobarbital and a 2% solution of Evans blue was injected into the RTN (50–75 nL). Saline followed by 4% buffered formalin (pH 7.4) was perfused through the heart. The brains were removed and processed as described previously (Wenker *et al.* 2013; Sobrinho *et al.* 2014). Injections sites in the RTN were confirmed by visual inspection using an Axioskop 2 microscope (Carl Zeiss, Oberkochen, Germany). Sections from different brains were aligned with respect to a reference section, which was the most caudal section containing an identifiable cluster of facial motor neurons. A value of 11.6 mm caudal to bregma (bregma -11.6 mm) (Paxinos & Watson, 1998) was assigned to this reference section. Levels rostral or caudal to this reference section were determined by adding or subtracting the number of intervening sections  $\times 40 \mu\text{m}$ .

PHA-L was detected using a polyclonal anti-PHA-L raised in goat (AS2224; dilution 1:5000; Vector Laboratories). Choline acetyltransferase (ChAT) was detected with a goat anti-ChAT antibody (AB 144P; dilution 1:500; Merck Millipore, Darmstadt, Germany).

All the primary antibodies were diluted in phosphate buffer (PB) containing 10% normal donkey serum (017-000-121; Jackson ImmunoResearch, West Grove, PA, USA) and 0.3% Triton X-100 and incubated for 24 h. Sections were subsequently rinsed in PB containing 1% normal donkey serum and incubated for 2 h in Alexa 594 donkey anti-goat (705-586-147; dilution 1:200; Jackson ImmunoResearch Laboratories) for PHA-L immunostaining, ChAT was revealed with Alexa 488 donkey anti-goat (705-546-147; dilution 1:200; Jackson ImmunoResearch Laboratories). The sections were mounted on gelatin-coated slides, coverslipped with Vectashield (Vector Laboratories) or DPX (Aldrich, Milwaukee, WI, USA) and sealed with nail polish.

Using the immunoperoxidase technique, PHA-L was detected with a polyclonal anti-PHA-L raised in goat (AS2224; dilution 1:5000; Vector Laboratories). Sections were incubated for 24 h at room temperature and diluted in PB containing 10% normal horse serum (008-000-001; Jackson ImmunoResearch Laboratories) and 0.3% Triton X-100. After several rinses, they were transferred to the appropriate affinity purified biotinylated secondary antibodies goat anti-rabbit (BA-1000; dilution 1:200; Vector Laboratories) for PHA-L; all diluted in TPB containing 1–10% normal horse serum and 0.3% Triton X-100 incubated for 24 h at room temperature, rinsed again and exposed to Extravidin (E2886; dilution 1:1000; Sigma-Aldrich) for 2 h 30 min at room temperature. Peroxidase reactions were visualized using

**Table 1. PHA-L-labelled varicosities within the brainstem**

Brainstem regions	PHA-L-labelled varicosities
Kölliker-Fuse	+++
Lateral parabrachial nucleus	+++
Parafacial respiratory group	++
Raphe pallidus	+++
Retrotrapezoid nucleus	++

+++; high expression, ++; moderate expression, +; low expression

the glucose oxidase procedure and 3,3'-diaminobenzidine tetrahydrochloride as chromogen for PHA-L. Sections were rinsed again in TPBS, mounted in sequential rostrocaudal order onto slides on gelatin-coated slides, dehydrated through a series of ascending concentrations of ethanol, transferred into xylene and coverslipped with DPX (06522; Sigma-Aldrich) for histology.

### Cell counting, imaging and data analysis

A multifunction microscope Axio Imager A1 microscope (Carl Zeiss) was used to image sections and perform the subsequent analysis. Immunofluorescence was examined under epifluorescence illumination and immunoperoxidase stained sections were examined under bright illumination.

The relative PHA-L in the RTN region was classified based on the relative density of the structure region containing PHA-L-immunoreactivity varicosities. Thus, the regions were classified as exhibiting high expression (+++), moderate expression (++) , low expression (+) and very low or virtually absent (–) (Table 1).

The locations of FG and ChAT immunoreactivity into the PPTg region were plotted in sections from 6.84 to 8.28 mm caudal to bregma (seven sections per animal). The locations of FG and ChAT immunoreactivity into the PiCO, nucleus ambiguus or dorsal motor nucleus of the vagus regions were plotted in sections from 11.86 to 13.3 mm caudal to bregma (seven sections per animal). To align sections around the Kölliker-Fuse region, the most rostral section featuring a cluster of facial motor neurons was identified in each brain, and assigned a level of 10.3 mm caudal to bregma, in accordance with the atlas of Paxinos and Watson (1998). Levels rostral or caudal to that reference section were defined by adding a distance corresponding to the interval between sections, multiplied by the number of intervening sections. The ventral quadrant of the side that received the tracer micro-injection was plotted, and profile counts reflect an average of the ipsilateral side of the brain.

Digital colour photomicrographs were acquired using a AxioCam HRc camera (Carl Zeiss). Images of double

immunoperoxidase and immunofluorescence stained sections were acquired and analysed with the Axiovision software (Carl Zeiss), which permits the acquisition of images from several separate fluorescence channels.

An LSM 780-NLO confocal microscope (Carl Zeiss) with a High Content Imaging In Cell Analyser 2200 (GE Healthcare Ltd, Little Chalfont, UK) was used to analyse PHA-L immunoreactivity in axonal varicosities located in the RTN region. PHA-L-labelled axonal varicosities were counted at five levels of the RTN. Image J, version 1.41 (NIMH, Bethesda, MD, USA) was used for cell counting and Canvas software, version 9.0 (ACD Systems, Victoria, BC, Canada) was used for line drawings. The neuroanatomical nomenclature employed during experimentation and in this manuscript was defined by Paxinos & Watson (1998).

### Statistical analysis

Excel 2010 (Microsoft Corp., Redmond, WA, USA) and Prism, version 6 (GraphPad Software, Inc., La Jolla, CA, USA) were used to collect and analyse data. The distribution of the data was tested for normality (Shapiro–Wilk normality test), and significant differences between samples were determined with one-way ANOVA (Kruskal–Wallis for non-Gaussian data) and Two-Way ANOVA and unpaired two-tailed *t* tests (Mann–Whitney test for non-Gaussian data). *P* < 0.05 was considered statistically significant. The results are presented as the mean ± SEM, unless noted otherwise.

## Results

### Cholinergic innervation of the RTN: physiological and anatomical evidence

The RTN receives cholinergic innervation as denoted by the presence of terminals that contained anti-ChAT immunoreactivity (Fig. 1A). To determine whether cholinergic transmission at the level of the RTN contributes to control of breathing, we injected ACh and/or the muscarinic receptor antagonist (M-Atr) into the RTN when measuring respiratory activity under control conditions and during exposure to 7% CO<sub>2</sub> (Figs 1 and 2). All RTN injections (uni- or bilateral) were placed 250 μm below the facial motor nucleus and 200 μm rostral to the caudal end of this nucleus to target the region containing the highest density of CO<sub>2</sub>-sensitive RTN neurons (Mulkey *et al.* 2004; Takakura & Moreira, 2011) (Figs 1C and 2B). Control injections were made more caudally to target presympathetic catecholaminergic (C1) neurons and expiratory Bötzing neurons (C1/BötC).

In the awake rats, injection of ACh into the RTN increased baseline breathing. For example, unilateral

RTN injection of ACh (10 mM in 50 nL,  $n = 5$ ) increased  $V_T$  [ $10.4 \pm 0.91$  vs. resting:  $7.8 \pm 0.9$  mL kg<sup>-1</sup>; one-way repeated measures (RM) ANOVA:  $F_{2,17} = 55.81$ ,  $P = 0.001$ ],  $f_R$  ( $154 \pm 8$  vs. resting:  $89 \pm 3$  breaths min<sup>-1</sup>; one-way RM ANOVA:  $F_{2,17} = 105.65$ ,  $P = 0.001$ ) and  $V_E$  ( $1528 \pm 114$  vs. resting:  $703 \pm 56$  mL kg<sup>-1</sup> min<sup>-1</sup>; one-way RM ANOVA:  $F_{2,17} = 94.32$ ,  $P = 0.001$ ) (Fig. 1B and D–F). Injections of ACh into the RTN also increased MAP ( $138 \pm 5$  vs. resting:  $104 \pm 4$  mmHg; one-way RM ANOVA:  $F_{2,17} = 73.46$ ,  $P = 0.012$ ), although with negligible effects on HR ( $328 \pm 10$  vs. resting:  $333 \pm 13$  mmHg; one-way RM ANOVA:  $F_{2,17} = 1.81$ ,  $P = 0.2$ ) (Fig. 1B and G).

Application of ACh into the nearby C1/BötC also increased cardiorespiratory output. In this case, ACh increased  $f_R$  ( $132 \pm 11$  vs. resting:  $88 \pm 6$  breaths min<sup>-1</sup>; one-way RM ANOVA:  $F_{2,32} = 52.11$ ,  $P = 0.0023$ ) but decreased  $V_T$  (one-way RM ANOVA:  $F_{2,32} = 63.15$ ,  $P = 0.015$ ). ACh also increased both MAP ( $156 \pm 11$  vs. saline:  $112 \pm 6$  mmHg; one-way RM ANOVA:  $F_{2,32} = 94.13$ ,  $P = 0.001$ ) and HR ( $378 \pm 18$  vs. saline:  $322 \pm 9$  breaths min<sup>-1</sup>; one-way RM ANOVA:  $F_{2,32} = 79.07$ ,  $P = 0.04$ ) (data not shown). As expected, ACh injections into the facial motor nucleus had no measurable effect on cardiorespiratory output (data not shown).

Injection of the muscarinic receptor antagonist M-Atr (5 mM/50–75 nL) into the RTN or C1/BötC eliminated breathing and blood pressure responses to exogenous ACh (Fig. 1B and D–G). Also, consistent with our previous work showing that CO<sub>2</sub>/H<sup>+</sup>-sensitivity of RTN neurons is not dependent on cholinergic signalling (Sobrinho *et al.* 2016), we found that RTN injections of M-Atr minimally affected baseline breathing or the CO<sub>2</sub> ventilatory response of awake rats (Fig. 2C–E). These results show that cholinergic transmission at the level of the RTN can stimulate cardiorespiratory activity in awake rats; however, cholinergic control of RTN chemoreception is not an essential component of the drive to breathe in the awake state.

We also found that, in the same group of animals, bilateral injections of M-Atr (5 mM/50–75 nL) into the RTN of urethane-anaesthetized animals caused a decrease in basal  $V_T$  ( $5.9 \pm 0.5$  vs. saline:  $7.6 \pm 0.6$  mL kg<sup>-1</sup>; two-way RM ANOVA:  $F_{1,34} = 145.74$ ;  $P = 0.022$ ),  $f_R$  ( $92 \pm 4$  vs. saline:  $101 \pm 6$  breaths min<sup>-1</sup>; two-way RM ANOVA:  $F_{1,34} = 44.28$ ;  $P = 0.03$ ) and  $V_E$  ( $553 \pm 47$  vs. saline:  $771 \pm 57$  mL kg<sup>-1</sup> min<sup>-1</sup>; two-way RM ANOVA:  $F_{1,34} = 126.18$ ;  $P = 0.035$ ) (Fig. 2F–H). This treatment also reduced the ventilatory response to CO<sub>2</sub>; M-Atr

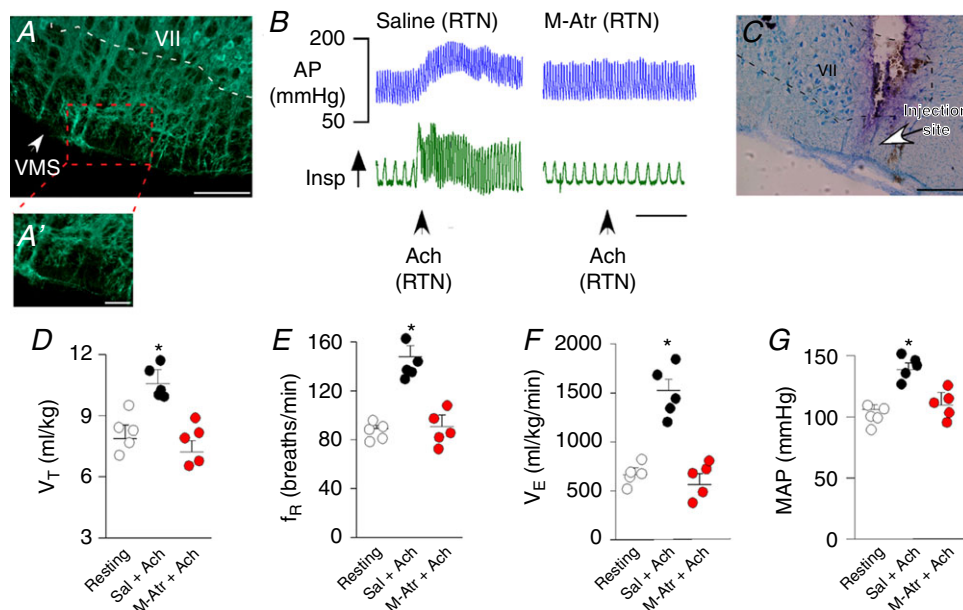


**Figure 1. Injection of ACh into the RTN increased breathing and blood pressure in awake unrestrained rats by a muscarinic cholinergic receptor-dependent mechanism**

A, histology section showing ChAT immunoreactivity at the level of the RTN region. B, cardiovascular and ventilatory responses elicited by ACh injection into the RTN of awake unrestrained rats before and after unilateral RTN injections of saline or M-Atr. C, histology section showing the location of drug injections within the RTN. D–G, summary data ( $n = 5$  rats) showing the effect of unilateral RTN injections of saline (Sal; 50–75 nL), ACh (10 mM/50 nL) and ACh plus M-Atr (5 mM/50–75 nL) on  $V_T$  (D);  $f_R$  (E);  $V_E$  (F); and MAP (G) in awake unrestrained rats. VII, facial motor nucleus; VMS, ventral medullary surface. Scale bar = 100  $\mu$ m in (A) and (C) and 50  $\mu$ m in (A'). \*Statistically different from both resting and M-Atr (one-way RM ANOVA with Bonferroni's correction for multiple comparisons). [Colour figure can be viewed at [wileyonlinelibrary.com](http://wileyonlinelibrary.com)]

decreased the CO<sub>2</sub>-evoked increase in  $V_T$  ( $8.4 \pm 0.9$  vs. saline:  $11.2 \pm 1$  mL kg<sup>-1</sup>; two-way RM ANOVA:  $F_{1,28} = 87.62$ ;  $P = 0.028$ ) and  $V_E$  ( $1067 \pm 52$  vs. saline:  $1436 \pm 144$  mL kg<sup>-1</sup> min<sup>-1</sup>; two-way RM ANOVA:  $F_{1,34} = 115.22$ ;  $P = 0.01$ ) (Fig. 2*F* and *H*). These results support the possibility that cholinergic transmission at the level of the RTN helps maintain breathing during states of reduced consciousness.

To identify the source of cholinergic input, the retrograde tracer FG 2% was injected by iontophoresis unilaterally under the caudal end of the facial motor nucleus in the dorsal cap region of the RTN ( $n = 4$ ) (Fig. 3*A* and *B*). Consistent with previous work from our laboratory (Silva *et al.* 2016*a*, 2016*b*), FG-labelled neurons were present in several brainstem respiratory

centres known to project to the RTN (e.g. nucleus of the solitary tract and Kölliker-Fuse region (Fig. 3*I*, *K*, *L* and *N*), thus giving us confidence that injections targeted RTN and were properly transported. Interestingly, we also identified a high number of FG-labelled neurons in the recently identified PiCO (Anderson *et al.* 2016) that were also immunoreactive for ChAT ( $95 \pm 5\%$ ), suggesting cholinergic input from the PiCO may also regulate RTN function (Fig. 3*F–H*). We also found a significant number of FG-labelled neurons in PPTg that were immunoreactive for ChAT ( $33 \pm 8\%$ ) (Fig. 4*A–G*). We did not find double-labelled neurons within the dorsal motor nucleus of the vagus or within the nucleus ambiguus (Fig. 3*C–E* and *I–K*). Taken together, these results identify the PPTg and PiCO as potential sources of cholinergic input to

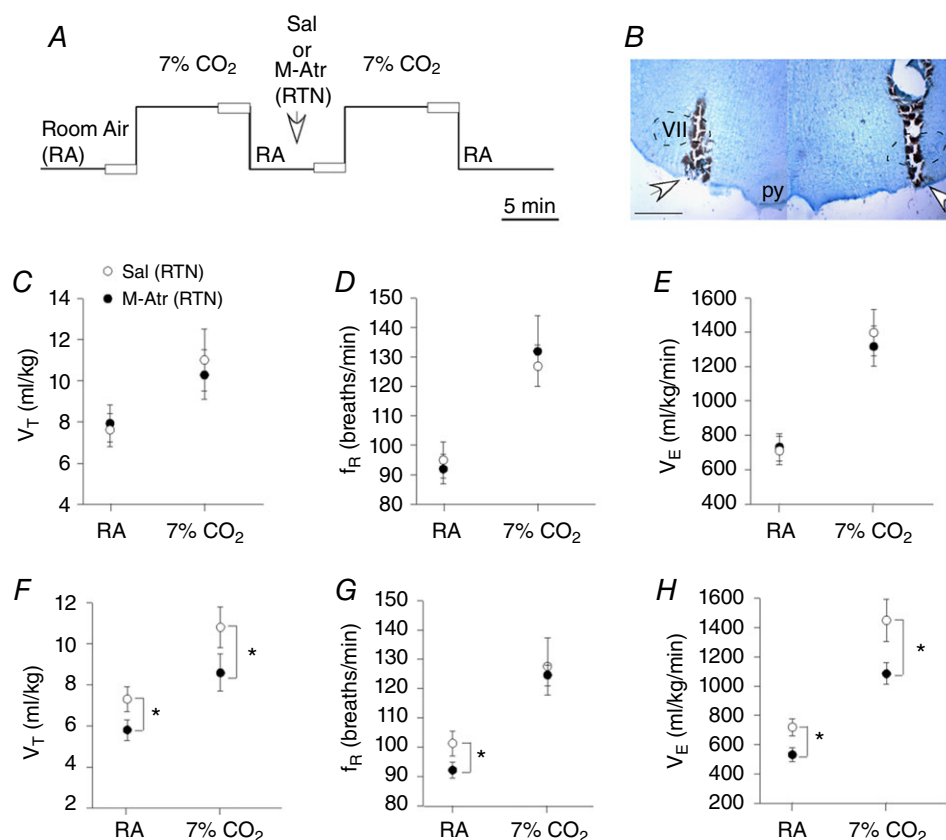


**Figure 2.** Effects of M-Atr injections into the RTN on baseline breathing and ventilatory response to CO<sub>2</sub>

*A*, experimental design used to assess CO<sub>2</sub> ventilatory responses by plethysmography of awake or anaesthetized rats before and after bilateral RTN injections of saline or M-Atr; open boxes during the last 2 min of each condition represent periods used for data analysis. *B*, histology section showing the location of the bilateral injection into the RTN. *C–E*, summary data ( $n = 6$  rats) from awake rats showing that bilateral RTN injections of saline or M-Atr (5 mM/50–75 nL) had negligible effects on  $V_T$  (*C*),  $f_R$  (*D*) or  $V_E$  (*E*). *F–H*, summary data ( $n = 6$  rats) from urethane (1.2 g kg<sup>-1</sup>) anaesthetized rats shows effects of bilateral RTN injections of saline or M-Atr on  $V_T$  (*C*),  $f_R$  (*D*) and  $V_E$  (*E*). M-Atr decreased baseline breathing and the ventilatory response to CO<sub>2</sub> in anaesthetized but not awake rats, thus demonstrating that cholinergic drive to the RTN helps maintain breathing during states of reduced consciousness. VII, facial motor nucleus; py, pyramidal tract. Scale bar = 1 mm. \*Statistically different from saline (control) (two-way RM ANOVA with Bonferroni's correction for multiple comparisons). [Colour figure can be viewed at [wileyonlinelibrary.com](http://wileyonlinelibrary.com)]



the RTN. Because connections between cholinergic PPTg neurons and the RTN may provide an anatomical basis for state-dependent control of breathing, for the remainder of the present study, we focused on the PPTg to determine whether cholinergic input from the PPTg to the RTN regulates breathing in awake animals.

To further explore this possibility, we performed a series of anterograde axonal tracing experiments by injecting

PHA-L into the PPTg. Four of seven injections were correctly placed in the PPTg (Fig. 5A and B). In each of these four cases, the PHA-L injection was centred at the level of the compact aspect of the PPTg (Bregma level = -7.8 mm). Non-branching fibres without evidence of terminal specializations are probably fibres of passage and were not documented in the present study. We focused on axonal varicosities that have a distinct globular

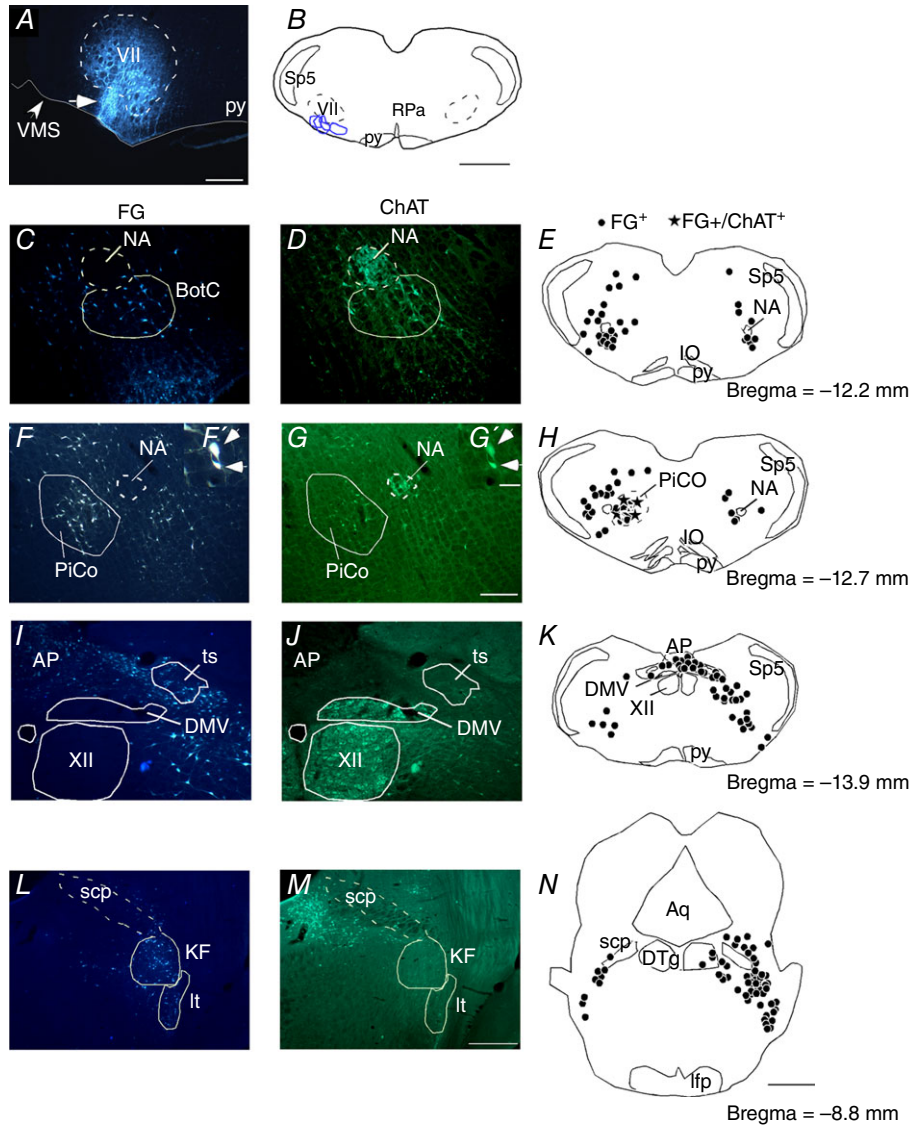


**Figure 3. Cholinergic inputs to the RTN**

A, photomicrography showing the location of an individual FG injection into the RTN. B, schematic drawing depicting the location of all FG injections into the RTN ( $n = 4$ ). C–N, FG injections into the RTN-labelled neurons that were immunoreactive for ChAT (ChAT-ir) in the nucleus ambiguus and Böttinger complex (NA–BötC) (C–E), PiCo (F–I), G–G' and H), dorsal motor nucleus of the vagus (DMV) (I–K) and intertrigeminal (It) and Kolliker-Fuse (KF) region (L–N). Aq, aqueduct mesencephalic; AP, area postrema; ts, solitary tract; BötC, Böttinger complex; cc, central canal; DTg, dorsal tegmental nucleus; it, intertrigeminal region; NA, nucleus ambiguus; XII, hypoglossal motor nucleus; scp, superior cerebellar peduncle; VMS, ventral medullary surface; VII, facial motor nucleus; XII, hypoglossal motor nucleus; Sp5, spinal trigeminal nucleus; RPa, raphe pallidus. Scale bar = 300  $\mu\text{m}$  in (A); 1 mm in (B) and (N); 100  $\mu\text{m}$  in (G) applied to (C) to (G); 20  $\mu\text{m}$  in (G') applied to (F') and (G') and 200  $\mu\text{m}$  in (M) applied to (I) to (M). [Colour figure can be viewed at [wileyonlinelibrary.com](http://wileyonlinelibrary.com)]

appearance and represent potential synapses (Fig. 5E and F). Light and electron microscopic analysis has already demonstrated that axonal varicosities observed by light microscopy are indeed terminal specializations forming synapses (Kincaid *et al.* 1998). Two weeks after injection, numerous PHA-L-labelled axonal terminals (putative synapses) were present in the RTN where chemosensitive neurons are localized (Mulkey *et al.* 2004; Takakura *et al.* 2006; Kumar *et al.* 2015). Figure 5C and D shows a photomicrograph and a computer-assisted plot of the PHA-L-labelled terminals that were detected in a representative coronal section located close to Bregma  $-11.4$  mm ( $200 \mu\text{m}$  rostral to the caudal end of the facial motor nucleus). The plotting was limited to the ventral third of the brain. PHA-L-labelled varicosities were found throughout the ventral medulla, albeit at variable densities. As shown in Fig. 5C–D, these putative synapses were especially numerous under the medial half of the facial motor nucleus in very close proximity to the ventral medullary surface. The numbers of PHA-L-labelled axonal

varicosities present within RTN (for details, see Methods) were counted in five equidistant sections per rat and the results are shown in Table 1. The area with the maximum density of varicosities corresponds to the region where we find the greatest concentration of  $\text{CO}_2$ -responsive neurons and the place where the retrograde tracer was injected. We also found a high number of PHA-L-labelled terminals within the Kölliker-Fuse/parabrachial complex and medullary raphe region (Fig. 5E–F and Table 1).

### Stimulation of the PPTg increases breathing activity through a cholinergic drive to the RTN in conscious rats

The PPTg is an important source of cholinergic drive to brainstem respiratory centres, including the RTN (Figs 4 and 5), and, because ACh strongly activates chemosensitive RTN neurons (Fig. 1) (Sobrinho *et al.* 2016), we next aimed to determine the effects of PPTg stimulation on respiratory output and whether cholinergic-dependent

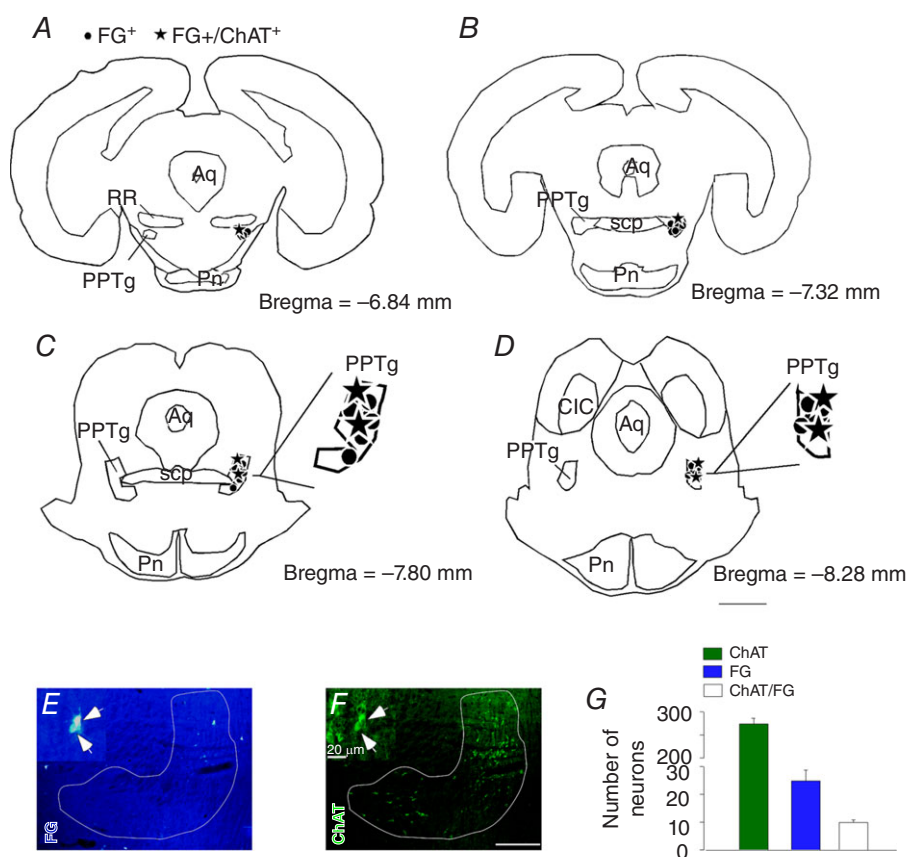


**Figure 4. Cholinergic projection from the PPTg to the RTN**

A–D, schematic drawing depicting the location of all FG-labelled cells and FG $^+$ /ChAT $^+$  cells through the PPTg region. E, photomicrograph showing retrograde FG tracer in the PPTg region. F, immunoreactivity for ChAT in the PPTg region. G, total number of PPTg neurons detected in four sections per brain (ChAT and FG only, FG $^+$ /ChAT $^+$ ). Aq, aqueduct mesencephalic; CIC, central inferior colliculus; PN, pontine nucleus; RR, retrorubral nucleus; scp, superior cerebellar peduncle. Scale bar = 2 mm in (D);  $100 \mu\text{m}$  in (F) applied to (E) and (F) and  $20 \mu\text{m}$  in (F) applied to (E) and (F). [Colour figure can be viewed at [wileyonlinelibrary.com](http://wileyonlinelibrary.com)]

signalling at the level of the RTN contributes to this response. By contrast to previous work showing that PPTg stimulation inhibits respiratory activity (Saponjic *et al.* 2005), we found that PPTg stimulation enhanced respiratory output in anaesthetized and awake rats. For example, under urethane anaesthesia, unilateral PPTg injection of glutamate (10 mM/100 nL) increased diaphragm frequency ( $\text{Dia}_{\text{EMG}}$  freq) by  $12.2 \pm 2\%$  ( $t$  test:  $t = 4.630$ ;  $P = 0.0012$ ), diaphragm amplitude ( $\text{Dia}_{\text{EMG}}$  amp) by  $12.8 \pm 3.5\%$  ( $t$  test:  $t = 0.2634$ ;  $P = 0.0272$ ) and genioglossus frequency ( $\text{GG}_{\text{EMG}}$  freq) by  $12.6 \pm 1.3\%$ , ( $t$  test:  $t = 5.943$ ;  $P = 0.0003$ ) (Fig. 6A–B, D and E). Stimulation of PPTg elicited a decrease in genioglossus amplitude ( $\text{GG}_{\text{EMG}}$  amp) by  $20.1 \pm 13.7\%$ , ( $t$  test:  $t = 1.7486$ ;  $P = 0.0357$ ) (Fig. 6A and C). We paralleled these experiments in unrestrained awake rats when monitoring respiratory activity by whole body plethysmography and found that glutamate injection into the PPTg also increased  $f_{\text{R}}$  ( $127 \pm 4.5$  vs. saline:  $86 \pm 3$  breaths  $\text{min}^{-1}$ ;  $t$  test:  $t = 7.56$ ;  $P < 0.0001$ ) and  $V_{\text{E}}$  ( $904 \pm 47$  vs. saline:  $745 \pm 44$  mL  $\text{kg}^{-1}$   $\text{min}^{-1}$ ;  $t$  test:  $t = 2.207$ ;  $P = 0.02$ ) (Fig. 7A, D–E), although in conjunction with a decrease in  $V_{\text{T}}$  ( $7.1 \pm 0.4$  vs. saline:  $8.6 \pm 0.3$  mL  $\text{kg}^{-1}$ ;  $t$  test:  $t = 2.887$ ;  $P = 0.0081$ ) (Fig. 7C).

To determine whether cholinergic signalling in the RTN contributes to the ventilatory response elicited by PPTg stimulation, we retested the effects of PPTg stimulation on breathing in awake rats after unilateral RTN injections of M-Atr. As noted above, RTN injection of M-Atr (5 mM/50–75 nL) had no effect on baseline respiratory activity in awake rats (Fig. 2). However, the increase in  $f_{\text{R}}$  ( $93 \pm 11$  vs. saline + glutamate:  $127 \pm 4.5$  breaths  $\text{min}^{-1}$ ; one-way RM ANOVA:  $F_{3,37} = 11.59$ ;  $P = 0.0001$ ) and  $V_{\text{E}}$  ( $774 \pm 122$  vs. saline + glutamate:  $945 \pm 44$  mL  $\text{kg}^{-1}$   $\text{min}^{-1}$ ; one-way RM ANOVA:  $F_{3,37} = 3.147$ ;  $P = 0.03$ ) elicited by glutamate injection into the PPTg in unrestrained awake rats was blunted by prior injection of M-Atr (5 mM/50–75 nL) into the medial RTN (Fig. 7B, D–E). The decrease in  $V_{\text{T}}$  ( $8.18 \pm 0.6$  vs. saline + glutamate:  $7.6 \pm 0.3$  mL  $\text{kg}^{-1}$   $\text{min}^{-1}$ ; one-way RM ANOVA:  $F_{3,37} = 3.066$ ;  $P = 0.03$ ) produced by glutamate into the PPTg was also blocked after M-Atr (5 mM/50–75 nL) into the RTN (Fig. 7C).

A subset of cholinergic neurons in the PPTg co-express the glutamatergic marker VGLUT2 (Luquin *et al.* 2018). We also tested the effects of PPTg stimulation on breathing in awake rats after unilateral RTN injections of the broad spectrum ionotropic glutamatergic receptors antagonist kyn (Fig. 7B). The injections were located in

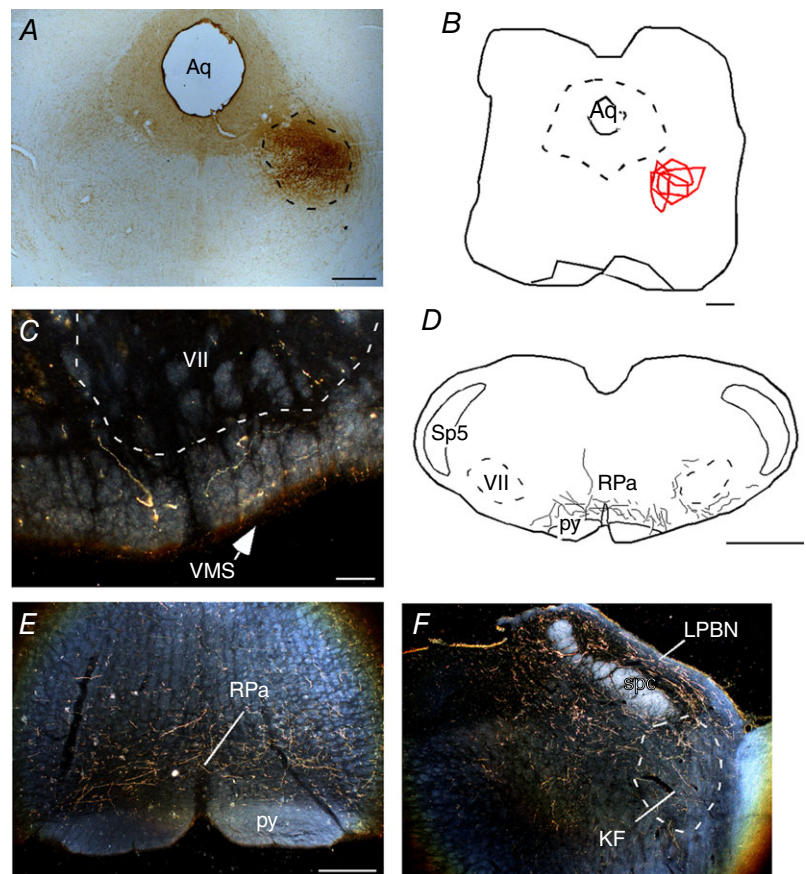


**Figure 5. Projection of the PPTg to the RTN**

A, photomicrograph showing the typical site anterograde neuronal tracer injection PHA-L in the PPTg. B, schematic drawing showing the location PHA-L injections ( $n = 4$ ) in the region of the PPTg. C, E and F, photomicrographs showing varicosities in the region of the RTN (C); raphe pallidus (E) and Kölliker-Fuse region (F). D, schematic drawing showing varicosities in RTN regions. Aq, aqueduct mesencephalic; KF, Kölliker-Fuse; LPBN, lateral parabrachial nucleus; py, pyramidal tract; RPa, raphe pallidus; scp, superior cerebellar peduncle; Sp5, spinal trigeminal nucleus; VMS, ventral medullary surface; VII, facial motor nucleus. Scale bar = 1 mm in (A), (B) and (D); 100  $\mu\text{m}$  in (C) and 300  $\mu\text{m}$  in (E) applied to (E) and (F). [Colour figure can be viewed at [wileyonlinelibrary.com](http://wileyonlinelibrary.com)]

a region close to ventral medullary surface (Fig. 7B). We found that unilateral injection of kyn into the RTN (100 mM/50–75 nL) had no effect on baseline respiratory activity (data not shown) (Moreira *et al.* 2006; Takakura *et al.* 2011) or the ventilatory response to PPTg stimulation (one-way RM ANOVA:  $F_{3,37} = 0.094$ ;  $P = 0.065$ ) (Fig. 7C–E). The dose of kyn used in the present study was based on previous work from our laboratory (Takakura and Moreira, 2011; Takakura *et al.* 2011) and the fact that kyn into the PPTg blocked the  $V_E$  ( $745 \pm 44$  vs. saline + glutamate  $945 \pm 28$  mL kg<sup>-1</sup> min<sup>-1</sup>;  $P > 0.05$ ) to glutamate injection into the PPTg (data not shown).

## Discussion

The present study provides a comprehensive description of the role of cholinergic signalling at the RTN region in the control of breathing output. We identify cholinergic PPTg neurons as an important source of ACh to the RTN, and we show that (i) RTN injections of ACh increased respiratory activity in anaesthetized and awake rats by a muscarinic receptor-dependent mechanism; (ii) muscarinic receptor blockade at the level of the RTN decreased basal breathing and CO<sub>2</sub>-sensitivity in urethane-anaesthetized but not awake rats; and (iii) cholinergic muscarinic receptors, but not ionotropic glutamatergic receptors, within the RTN mediate most of the ventilatory response to PPTg stimulation. Based on previous evidence that cholinergic PPTg projections may simultaneously activate expiratory

output from the pFRG, we speculate that cholinergic signalling at the level of RTN region could also be involved in breathing regulation.

## Cholinergic signalling in the RTN in the regulation of breathing

PPTg has around 3000 cholinergic neurons (Mena-Segovia and Bolam, 2017; Luquin *et al.* 2018) that exhibit extensive dendritic arborization, where the major branch splits until six collaterals that are directed to forebrain and rhombencephalon (Mena-Segovia *et al.* 2008). In the present study, we confirmed previous evidence indicating that one of the major source of cholinergic drive to the ventral lateral medulla, including the RTN region, comes from cholinergic PPTg neurons (Yasui *et al.* 1990). These neurons exhibit wake- and REM-dependent firing behaviour (Kubin & Fenik, 2004) and are known to participate in a wide range of state-regulating functions, including the control of breathing (Lydic & Baghdoyan, 1993; Saponjic *et al.* 2003; Boutin *et al.* 2017). Consistent with previous work (Saponjic *et al.* 2003, 2005; Topchiy *et al.* 2010), we found that that stimulation of PPTg region with glutamate elicited an increase in ventilation. This ventilatory response could be blocked by prior RTN injection of M-Atr but not kyn. Therefore, we demonstrated for the first time using standard neuroanatomical and physiological approaches that the increase in breathing elicited by PPTg stimulation is dependent on a cholinergic signalling

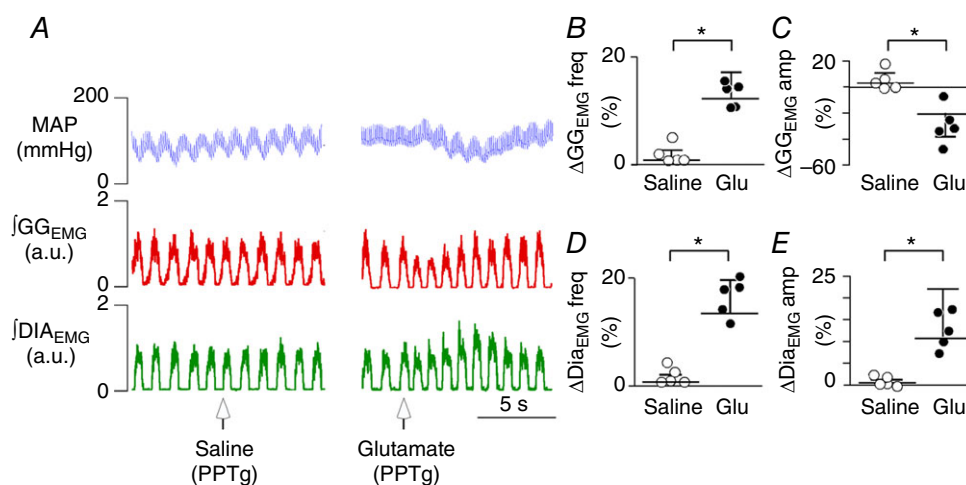


**Figure 6.** Respiratory effects produced by the unilateral injection of glutamate in the PPTg in anaesthetized rats

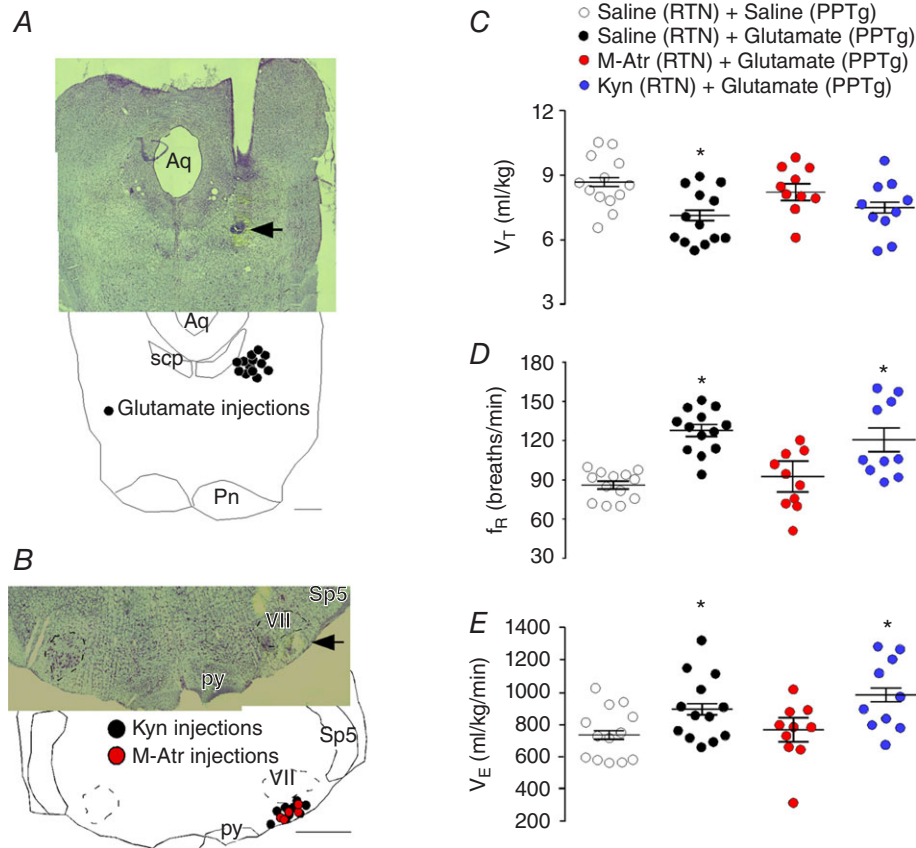
A, illustrative image showing respiratory changes observed after the application of glutamate in the PPTg region. B–E, summary data ( $n = 5$  rats per group) showing the effect of unilateral PPTg injections of saline (Sal; 100 nL) or glutamate (Glu; 10 mM/100 nL) on genioglossal frequency (GG<sub>EMG</sub> freq) (B); genioglossal amplitude (GG<sub>EMG</sub> amp) (C); diaphragm frequency (Dia<sub>EMG</sub> freq) (D); and diaphragm amplitude (Dia<sub>EMG</sub> amp) (E). \*Statistically different from saline control. [Colour figure can be viewed at [wileyonlinelibrary.com](http://wileyonlinelibrary.com)]

via the medial aspect of the RTN. Connections between cholinergic PPTg neurons and RTN chemoreceptors may serve as the anatomical basis for state-dependent control of chemoreceptor activity.

According to the present study, stimulation of PPTg also produced a reduction in genioglossus muscle activity, suggesting that the PPTg differentially regulates respiratory drive across the respiratory circuit. Although this response is consistent with previous work showing that ACh can inhibit activity of hypoglossal motor neurons that maintain genioglossus muscle activity (Bellingham and Berger, 1996; Ireland *et al.* 2012), this response would also favour airway collapse during inspiration and so may contribute to the inhibitory effects of PPTg stimulation of tidal volume. At levels of the respiratory system upstream of motor neurons, ACh is generally excitatory and, because PPTg neurons innervate many brainstem structures including pontine respiratory centres

associated with expiration (e.g. parabrachial complex and Kölliker-Fuse), PPTg cholinergic neurons mediating respiratory depression and variability probably results from cholinergic activation of expiratory drive (Saponjic *et al.* 2006; Boutin *et al.* 2017). Consistent with this possibility, we show that ACh injections into another expiratory region, the C1/Bötzinger region, decreased respiratory activity and increased blood pressure in awake rats, presumably by activation of expiratory and pre-sympathetic neurons, respectively. To fully understand the contribution of cholinergic drive to state-dependent control of breathing, it will be important for future work to identify and selectively manipulate subsets of cholinergic PPTg neurons with discrete projections to various levels of the respiratory system across natural sleep-wake states.

The RTN is located in close proximity to C1 and non-C1 neurons that regulate blood pressure (Padley *et al.*



2007; Wenker *et al.* 2013, 2017) and there is evidence to suggest that cholinergic drive to these cells increases blood pressure and contributes to the pathogenesis of hypertension (Kubo, 1998; Padley *et al.* 2007). Consistent with this evidence, we show that RTN injection of ACh increased respiratory activity in awake unrestrained rats. We also found that ACh increased blood pressure and heart rate and M-Atr blocked these cardiorespiratory responses. Interestingly, application of M-Atr into the RTN decreased basal breathing and the CO<sub>2</sub> ventilatory response of urethane-anaesthetized but not awake rats. Consistent with our data from awake rats, we show that, at the cellular level, muscarinic receptor blockade had negligible effect on CO<sub>2</sub>/H<sup>+</sup>-sensitivity of RTN chemoreceptors. Taken together, these results indicate that cholinergic signalling can modulate activity of RTN neurons and serve to maintain breathing during states of reduced consciousness, although it is not a requisite component of the mechanism by which these cells sense changes in CO<sub>2</sub>/H<sup>+</sup>.

### Cholinergic pathway from postinspiratory complex to RTN region

The PiCO was recently identified as a key region for the generation of postinspiratory activity (Anderson *et al.* 2016). This region is located dorsomedial to the nucleus ambiguus and contains neurons that co-express glutamate and ACh. PiCO neurons display autonomous postinspiratory bursts always, although not inspiratory related activity (Anderson *et al.* 2016; Ramirez *et al.* 2016). In addition, selective stimulation of the RTN region increased breathing by shortening postinspiratory activity (Burke *et al.* 2015). Both regions have a role in post-inspiratory activity; a considerable number of cholinergic neurons within the PiCO have projections to the RTN (present study; Fig. 3F–H); and cholinergic mechanisms could also play an important role for the generation of active expiration during sleep (Boutin *et al.* 2017). An excitatory cholinergic input from PiCO to RTN cells should also theoretically be able to control postinspiratory activity. Taken together, the evidence indicates that the three respiratory oscillators are interconnected (Anderson *et al.* 2016; Anderson & Ramirez, 2017; Boutin *et al.* 2017; present study) and RTN have an involvement in the three phases of the respiratory cycle. Further studies will be necessary to investigate the physiological role of direct cholinergic projections from PiCO to RTN neurons in breathing control.

### Conclusions

In summary, we show that ACh modulates respiratory output at RTN level and provide anatomical and physio-

logical evidences that this modulation is mediated by the mesopontine region PPTg. Additionally, we also provide the first anatomical evidence that RTN receive cholinergic inputs from PiCO, for which the functional role remains to be clarified. These results corroborate with a previous study from our group (Sobrinho *et al.* 2016) showing that ACh modulates RTN chemoreceptors by mechanisms involving M1 and M3 receptors and Gq mediated inhibition of KCNQ channels, and that these mechanisms could provide potential avenues for the therapeutic treatment of respiratory control problems associated with sleep disordered breathing.

### References

- Anderson TM, Garcia AJ, Baertsch NA, Pollak J, Bloom JC, Wei AD, Rai KG & Ramirez J-M (2016). A novel excitatory network for the control of breathing. *Nature* **536**, 76–80.
- Anderson TM & Ramirez J-M (2017). Respiratory rhythm generation: triple oscillator hypothesis. *F1000Research* **6**, 139.
- Barna BF, Takakura AC & Moreira TS (2014). Acute exercise-induced activation of Phox2b-expressing neurons of the retrotrapezoid nucleus in rats may involve the hypothalamus. *Neuroscience* **258**, 355–363.
- Barna BF, Takakura AC, Mulkey DK & Moreira TS (2016). Purinergic receptor blockade in the retrotrapezoid nucleus attenuates the respiratory chemoreflexes in awake rats. *Acta Physiol (Oxf)* **217**, 80–93.
- Bellingham MC, Berger AJ (1996). Presynaptic depression of excitatory synaptic inputs to rat hypoglossal motoneurons by muscarinic M2 receptors. *J Neurophysiol.* **76**, 3758–3770.
- Boutin RCT, Alshafi Z & Pagliardini S (2017). Cholinergic modulation of the parafacial respiratory group. *J Physiol* **595**, 1377–1392.
- Burke PGR, Kanbar R, Basting TM, Hodges WM, Viar KE, Stornetta RL & Guyenet PG (2015). State-dependent control of breathing by the retrotrapezoid nucleus. *J Physiol* **593**, 2909–2926.
- Burton MD, Nouri K, Baichoo S, Samuels-Toyloy N & Kazemi H (1994). Ventilatory output and acetylcholine: perturbations in release and muscarinic receptor activation. *J Appl Physiol* **77**, 2275–2284.
- Dev NB & Loeschcke HH (1979). A cholinergic mechanism involved in the respiratory chemosensitivity of the medulla oblongata in the cat. *Pflugers Arch* **379**, 29–36.
- Drorbaugh JE & Fenn WO (1955). A barometric method for measuring ventilation in newborn infants. *Pediatrics* **16**, 81–87.
- Fukuda Y & Loeschcke HH (1979). A cholinergic mechanism involved in the neuronal excitation by H<sup>+</sup> in the respiratory chemosensitive structures of the ventral medulla oblongata of rats in vitro. *Pflugers Arch* **379**, 125–135.
- Furuya WI, Bassi M, Menani J V., Colombari E, Zoccal DB & Colombari DSA (2014). Differential modulation of sympathetic and respiratory activities by cholinergic mechanisms in the nucleus of the solitary tract in rats. *Exp Physiol* **99**, 743–758.

- Grundy D (2015). Principles and standards for reporting animal experiments in *The Journal of Physiology and Experimental Physiology*. *Exp Physiol* **100**, 755–758.
- Guyenet PG & Bayliss DA (2015). Neural control of breathing and CO<sub>2</sub> homeostasis. *Neuron* **87**, 946–961.
- Huckstepp RTR, Cardoza KP, Henderson LE & Feldman JL (2018). Distinct parafacial regions in control of breathing in adult rats. *PLoS ONE* **13**, e0201485.
- Huckstepp RTR, Llaudet E & Gourine AV. (2016). CO<sub>2</sub>-induced ATP-dependent release of acetylcholine on the ventral surface of the medulla oblongata. *PLoS ONE* **11**, e0167861.
- Ireland MF, Funk GD, Bellingham MC (2012). Muscarinic acetylcholine receptors enhance neonatal mouse hypoglossal motoneuron excitability in vitro. *J Appl Physiol (1985)*. **113**, 1024–1039.
- Kincaid AE, Zheng T & Wilson CJ (1998). Connectivity and convergence of single corticostriatal axons. *J Neurosci* **18**, 4722–4731.
- Kubin L & Fenik V (2004). Pontine cholinergic mechanisms and their impact on respiratory regulation. *Respir Physiol Neurobiol* **143**, 235–249.
- Kubo T (1998). Cholinergic mechanism and blood pressure regulation in the central nervous system. *Brain Res Bull* **46**, 475–481.
- Kumar NN, Velic A, Soliz J, Shi Y, Li K, Wang S, Weaver JL, Sen J, Abbott SB, Lazarenko RM, Ludwig MG, Perez-Reyes E, Mohebbi N, Bettoni C, Gassmann M, Suply T, Seuwen K, Guyenet PG, Wagner CA & Bayliss DA (2015). Regulation of breathing by CO<sub>2</sub> requires the proton-activated receptor GPR4 in retrotrapezoid nucleus neurons. *Science (80-)* **348**, 1255–1260.
- Luquin E, Huerta I, Aymerich MS & Mengual E (2018). Stereological estimates of glutamatergic, GABAergic, and cholinergic neurons in the pedunculopontine and laterodorsal tegmental nuclei in the rat. *Front Neuroanat* **12**, 1–19.
- Lydic R & Baghdoyan HA (1993). Pedunculopontine stimulation alters respiration and increases ACh release in the pontine reticular formation. *Am J Physiol Regul Integr Comp Physiol* **264**, R544–R554.
- Mena-Segovia J, Sims HM, Magill PJ & Bolam JP (2008). Cholinergic brainstem neurons modulate cortical gamma activity during slow oscillations. *J Physiol* **586**, 2947–2960.
- Mena-Segovia J & Bolam JP (2017). Rethinking the pedunculopontine nucleus: from cellular organization to function. *Neuron* **94**, 7–18.
- Metz B (1966). Hypercapnia and acetylcholine release from the cerebral cortex and medulla. *J Physiol* **186**, 321–332.
- Monteau R, Morin D & Hilaire G (1990). Acetylcholine and central chemosensitivity: in vitro study in the newborn rat. *Respir Physiol* **81**, 241–253.
- Moreira TS, Takakura AC, Colombari E & Guyenet PG (2006). Central chemoreceptors and sympathetic vasomotor outflow. *J Physiol* **577**, 369–386.
- Mulkey DK, Stornetta RL, Weston MC, Simmons JR, Parker A, Bayliss DA & Guyenet PG (2004). Respiratory control by ventral surface chemoreceptor neurons in rats. *Nat Neurosci* **7**, 1360–1369.
- Nattie EE, Wood J, Mega A & Goritski W (1989). Rostral ventrolateral medulla muscarinic receptor involvement in central ventilatory chemosensitivity. *J Appl Physiol* **66**, 1462–1470.
- Del Negro CA, Funk GD & Feldman JL (2018). Breathing matters. *Nat Rev Neurosci* **19**, 351–367.
- Padley JR, Kumar NN, Li Q, Nguyen TBV, Pilowsky PM & Goodchild AK (2007). Central command regulation of circulatory function mediated by descending pontine cholinergic inputs to sympathoexcitatory rostral ventrolateral medulla neurons. *Circ Res* **100**, 284–291.
- Paxinos J & Watson C (1998). *The Rat Brain in Stereotaxic Coordinates*, 4th edn. Academic Press, San Diego, CA.
- Ramirez J-M, Dashevskiy T, Marlin IA & Baertsch N (2016). Microcircuits in respiratory rhythm generation: commonalities with other rhythm generating networks and evolutionary perspectives. *Curr Opin Neurobiol* **41**, 53–61.
- Ruggiero DA, Giuliano R, Anwar M, Stornetta R & Reis DJ (1990). Anatomical substrates of cholinergic-autonomic regulation in the rat. *J Comp Neurol* **292**, 1–53.
- Saponjic J, Radulovacki M & Carley DW (2003). Respiratory pattern modulation by the pedunculopontine tegmental nucleus. *Respir Physiol Neurobiol* **138**, 223–237.
- Saponjic J, Radulovacki M & Carley DW (2005). Injection of glutamate into the pedunculopontine tegmental nuclei of anesthetized rat causes respiratory dysrhythmia and alters EEG and EMG power. *Sleep Breath* **9**, 82–91.
- Saponjic J, Radulovacki M & Carley DW (2006). Modulation of respiratory pattern and upper airway muscle activity by the pedunculopontine tegmentum: role of NMDA receptors. *Sleep Breath* **10**, 195–202.
- Shao XM & Feldman JL (2009). Central cholinergic regulation of respiration: nicotinic receptors. *Acta Pharmacol Sin* **30**, 761–770.
- Silva JN, Lucena EV, Silva TM, Damasceno RS, Takakura AC & Moreira TS (2016a). Inhibition of the pontine Kölliker-Fuse nucleus reduces genioglossal activity elicited by stimulation of the retrotrapezoid chemoreceptor neurons. *Neuroscience* **328**, 9–21.
- Silva JN, Tanabe FM, Moreira TS & Takakura AC (2016b). Neuroanatomical and physiological evidence that the retrotrapezoid nucleus/parafacial region regulates expiration in adult rats. *Respir Physiol Neurobiol* **227**, 9–22.
- Sobrinho CR, Kuo F-S, Barna BF, Moreira TS & Mulkey DK (2016). Cholinergic control of ventral surface chemoreceptors involves Gq/inositol 1,4,5-trisphosphate-mediated inhibition of KCNQ channels. *J Physiol* **594**, 407–419.
- Sobrinho CR, Wenker IC, Poss EM, Takakura AC, Moreira TS & Mulkey DK (2014). Purinergic signalling contributes to chemoreception in the retrotrapezoid nucleus but not the nucleus of the solitary tract or medullary raphe. *J Physiol* **592**, 1309–1323.
- Takakura AC, Barna BF, Cruz JC, Colombari E & Moreira TS (2014). Phox2b-expressing retrotrapezoid neurons and the integration of central and peripheral chemosensory control of breathing in conscious rats. *Exp Physiol* **99**, 571–585.

- Takakura AC, Colombari E, Menani J V & Moreira TS (2011). Ventrolateral medulla mechanisms involved in cardiorespiratory responses to central chemoreceptor activation in rats. *Am J Physiol Regul Integr Comp Physiol* **300**, R501–R510.
- Takakura AC & Moreira TS (2011). Contribution of excitatory amino acid receptors of the retrotrapezoid nucleus to the sympathetic chemoreflex in rats. *Exp Physiol* **96**, 989–999.
- Takakura ACT, Moreira TS, Colombari E, West GH, Stornetta RL & Guyenet PG (2006). Peripheral chemoreceptor inputs to retrotrapezoid nucleus (RTN) CO<sub>2</sub>-sensitive neurons in rats. *J Physiol* **572**, 503–523.
- Topchiiy I, Waxman J, Radulovacki M & Carley DW (2010). Functional topography of respiratory, cardiovascular and pontine-wave responses to glutamate microstimulation of the pedunculopontine tegmentum of the rat. *Respir Physiol Neurobiol* **173**, 64–70.
- Wenker IC, Abe C, Viar KE, Stornetta DS, Stornetta RL & Guyenet PG (2017). Blood pressure regulation by the rostral ventrolateral medulla in conscious rats: effects of hypoxia, hypercapnia, baroreceptor denervation, and anesthesia. *J Neurosci* **37**, 4565–4583.
- Wenker IC, Sobrinho CR, Takakura AC, Moreira TS & Mulkey DK (2012). Regulation of ventral surface CO<sub>2</sub>/H<sup>+</sup>-sensitive neurons by purinergic signalling. *J Physiol* **590**, 2137–2150.
- Wenker IC, Sobrinho CR, Takakura AC, Mulkey DK & Moreira TS (2013). P2Y1 receptors expressed by C1 neurons determine peripheral chemoreceptor modulation of breathing, sympathetic activity, and blood pressure. *Hypertension* **62**, 263–273.
- Yasui Y, Cechetto DF & Saper CB (1990). Evidence for a cholinergic projection from the pedunculopontine tegmental nucleus to the rostral ventrolateral medulla in the rat. *Brain Res* **517**, 19–24.

## Additional information

### Competing interests

The authors declare that they have no competing interests.

### Author contributions

JDL, CRS, BF, ACT, DKM and TSM designed the research. JDL, CRS, BF, LKS and TSM performed the research. JDL, CRS, BF and TSM analysed data. JDL, CRS, ACT, DKM and TSM wrote the paper. JDL, CRS, BF, ACT, DKM and TSM performed a critical review of the manuscript. All authors approved the final version of the manuscript and agree to be accountable for all aspects of the work in ensuring that questions related to the accuracy or integrity of any part of the work are appropriately investigated and resolved. All persons designated as authors qualify for authorship, and all those who qualify for authorship are listed.

### Funding

This work was supported by the São Paulo Research Foundation (FAPESP; grants: 2016/23281-3 to ACT; 2015/23376-1 and 2016/22069-0 to TSM). FAPESP fellowship (2017/01380-2 to JDL; 2015/12827-2 to CRS); CNPq fellowship (301219/2016-8 to ACT and 301904/2015-4 to TSM). NIH/NHLBI grants HL104101, HL137094 to DKM. This work was also supported by a grant from the Dravet Foundation to DKM.

### Acknowledgements

We thank Claudio L. Castro, Phelipe E. Silva and Felipe C Souza for their excellent technical assistance.